Advances in Materials, Manufacturing, and Repair for Power Plants:
Proceedings from the Tenth International Conference
October 15–18, 2024, Bonita Springs Florida, USA
https://doi.org/10.31399/asm.cp.epri2024p0960

NONDESTRUCTIVE DETECTION OF CREEP DAMAGE IN ASME GRADE 91 STEEL WELDS

Kota Sawada [(1)]***; Yasushi Taniuchi*** [(1)]***; Takehiro Nojima*** [(1)]***; Kazuhiro Kimura*** [(1)]
Takahiro Kimura [(2)]***; Kyohei Nomura*** [(2)]***; Noriko Saito*** [(2)]***; Akira Morita*** [(3)]
Hiroyuki Hayakawa [(4)]***; Takao Sugiuchi*** [(5)]***; Kazushige Ohbitsu*** [(5)]
Masatsugu Yaguchi [(6)]***; Koju Nishizawa*** [(7)]***; Hiroshi Ozaki*** [(7)]
Hayato Fukunishi [(7)]***; Kouji Ohi*** [(8)]***; Tomoya Nishioka*** [(9)]
Naoya Emi [(9)]***; Hirokazu Okada*** [(9)]***; Nobuyoshi Komai*** [(10)]
Kyohei Hayashi [(10)]***; Kimihiko Tominaga*** [(10)]

(1) National Institute for Materials Science, Tsukuba, Japan
(2) IHI Corporation, Yokohama, Japan
(3) The Kansai Electric Power Co., Inc., Osaka, Japan
(4) Kyushu Electric Power Co., Inc., Fukuoka, Japan
(5) The Chugoku Electric Power Co., Inc., Higashihiroshima, Japan
(6) Central Research Institute of Electric Power Industry, Yokosuka, Japan
(7) Tokyo Electric Power Company Holdings, Inc., Yokohama, Japan
(8) Tokyo Power Technology Ltd., Kawasaki, Japan
(9) Nippon Steel Technology Co., Ltd., Amagasaki, Japan
(10) Mitsubishi Heavy Industries Ltd., Nagasaki, Japan

ABSTRACT

Nondestructive phased array ultrasonic testing (PAUT), eddy current testing with a high-temperature superconductor, direct current, and superconducting quantum interference device (ECT• HTS-dc-SQUID) and observation of a replica were conducted to detect creep damage of Grade 91 steel welds. Creep strain measurements were also performed for residual life assessment of the welds. PAUT showed that the threshold of creep damage detection was between 60% and 80% of the creep life. In the case of ECT• HTS-dc-SQUID, the threshold was between 80% and 90% of the creep life. Creep voids were observed on the replica just before creep rupture. A capacitive strain sensor, laser displacement meter, and SPICA strain measurement were used to detect changes in the strain during creep exposure. The capacitive strain sensor can continuously measure the strain during creep exposure. The laser displacement meter was used after creep interruption. Creep curves obtained by the capacitive strain sensor and laser displacement meter were similar to those obtained by the conventional extensometer with a linear gauge. The SPICA method successfully measured the strain in the heat-affected zone (HAZ) after creep exposure. The strain measured by SPICA was higher in HAZ than in the base and weld metal after creep exposure. Furthermore, the strain measured by SPICA in HAZ monotonously increased during creep exposure.

INTRODUCTION

In ultra-supercritical (USC) power plants, ASME Grade 91 steels are widely used for components such as pipes and tubes. Residual life assessment of the components is needed because in some cases, the operation time of the USC power plant is already more than 200,000 h [1]. The allowable stress has been reviewed for Grade 91 steels due to creep strength degradation in the long term [2, 3]. In the ASME code, the chemical compositions of Grade 91 steel were reviewed, leading to the specification of Type 2 [4]. The creep strength of Grade 91 steel welds is lower

than that of the base metal due to the remarkable degradation and damage during creep exposure for the welds compared to the base metal [5]. Therefore, residual life assessment should be performed based on the measurement of degradation and damage.

For Grade 91 steel welds, creep voids and cracks are formed in the fine-grained heat-affected zone (FGHAZ) in the long term, causing Type IV fracture [6]. Many researchers have tried to detect the creep voids and cracks in FGHAZ by nondestructive methods [7-9]. However, it is difficult to compare their methods due to the different specimens in their results. In the present study, several nondestructive methods were applied to the same Grade 91 steel weld specimens to establish a residual life assessment based on the validity of each method.

EXPERIMENTAL PROCEDURES

ASME SA-335M P91 (OD: 356 mm, WT: 50 mm) was used for the present study. The chemical compositions and heat treatment conditions of the steel are listed in Table 1. Heat treatment equivalent to stress relief annealing at 760°C for 2 h was carried out on the steel, and welding was carried out using tungsten inert gas (TIG; 1 or 2 layers) + shielded metal arc welding (SMAW; residual layer) on the weld material of the chemical compositions in Table 2, after which post-welding heat treatment at 760°C for 2 h was carried out. That is, the base metal part was subjected to heat treatment twice, and the weld part was subjected to heat treatment once after welding. Creep specimens were sampled from the girth weld joint. The weld metal was located at the center of the gauge portion of the creep specimens. The appearance of a creep specimen is shown in Fig. 1 The cross-section size of the gauge portion was 48×25 mm and the gauge length was 200 mm. Creep interrupted tests were performed at 625°C under 60 MPa. PAUT (transverse wave, 5 to 10MHz, sector scan) and ECT•HTS-dc-SQUID (excitation frequency :25Hz, measurement speed :10mm/sec, measurement interval :1mmStep, lift-off between ECT coil and test piece :about 0.5mm) were used to detect creep damage such as cracks. A replica obtained from the surface of the creep specimen was observed by optical microscopy (OM) and atomic force microscopy (AFM) to detect creep voids. The strain was measured by an extensometer for high-temperature use, a capacitive strain sensor, and a laser displacement meter. SPICA strain (digital image correlation technique for speckle pattern) was also evaluated by using platinum markers (size : 10mm x 15mm) attached to the surface of the creep specimen. Three specimens were used for the same creep conditions. Table 3 shows the inspection method for each specimen.

Table 1 Chemical compositions(mass%) and heat treatment conditions of steel examined.

C	Si	Mn	P	S	Ni	Cr	Mo	V
0.10	0.29	0.45	0.014	0.002	0.17	8.56	0.85	0.208

Nb	Al	N	Ti	Zr	Normalizing	Tempering
0.077	0.003	0.0375	< 0.003	< 0.001	1050°C, 10min A.C.	785°C, 45min A.C.

Table 2 Chemical compositions(mass%) of welding wire.

	C	Si	Mn	P	S	Cu	Ni	Cr
TIG	0.12	0.26	0.75	0.003	0.004	0.01	0.49	9.25
SMAW	0.10	0.28	0.85	<0.01	<0.01	0.02	0.43	8.9

Mo	V	Al	Nb	N
1.01	0.25	<0.01	0.06	0.04
1.04	0.22	<0.01	0.04	0.03

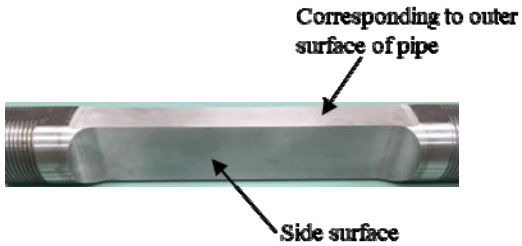

Figure 1 Appearance of creep specimen.

Table 3 Inspection methods for each specimen.

Specimen No.	Inspection method
1-2	Strain measurement : extensometer, capacitive strain sensor, laser displacement meter, SPICA
2-2	PAUT, OM and AFM for replica
3-2	PAUT, ECT・HTS-dc-SQUID, OM for replica

RESULTS and DISCUSSION

Type of creep damage

The appearance of a specimen just before creep rupture is shown in Fig. 2. A crack is clearly observed at the side surface of the specimen. Figure 3 shows the crack detection results obtained by PAUT. The results show that the crack is clearly detected in HAZ. The length of the crack was about half the thickness of the gauge portion. The crack was also observed inside the specimen shown in Fig. 3. The length of the crack was about 10 mm at the side surface shown in Fig. 2 However, the length of the crack was 23 mm at the center of the specimen thickness shown in Fig. 3. Therefore, the creep damage was larger on the inside than at the surface. The location of the crack was around the boundary between HAZ and the base metal, indicating Type IV fracture. It was confirmed by optical microscopy that many creep voids were observed in HAZ. Figure 4 shows the distribution of the creep void density in HAZ. The number of creep voids was a maximum at a depth of about 4 mm from the specimen surface corresponding to the outer surface of the pipe. On the other hand, the number of creep voids was low near the inner surface.

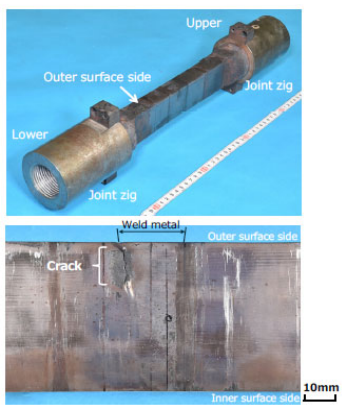

Figure 2 Appearance of specimen just before creep rupture.

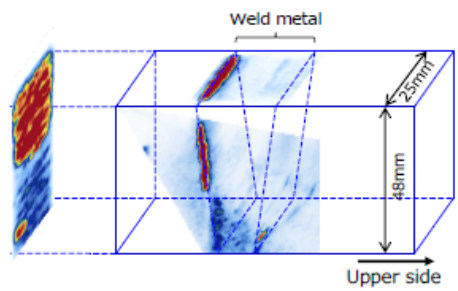

Figure 3 Crack detection results by PAUT just before creep rupture.

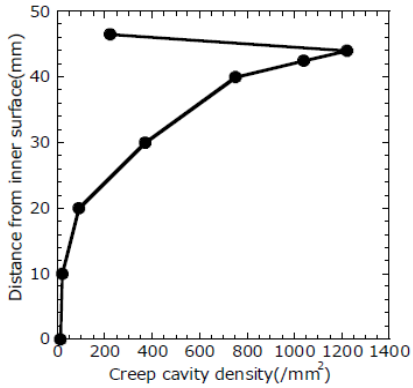

Figure 4 Distribution of creep void density in HAZ.

Nondestructive testing

Figure 5 shows the results of PAUT on the side surface of the creep interrupted specimens. Several indications were observed in the weld metal and fusion boundary. However, these indications were not creep damage because they were already detected before creep exposure. They may have been introduced during welding. Additionally, no large change in these indications occurred during creep exposure. On the other hand, another indication was detected in the HAZ of the specimens interrupted for 10,800 h and 12,215 h as indicated by the arrows. These are clearly creep damage indications because no indications were observed in the same location for the specimen interrupted for 7,800 h. Therefore, these indications were at least formed between 7,800 and 10,800 h corresponding to 57% and 79% of the creep life, respectively. For another specimen in this study, the creep damage in HAZ was detected between 63% and 87% of the creep life by PAUT.

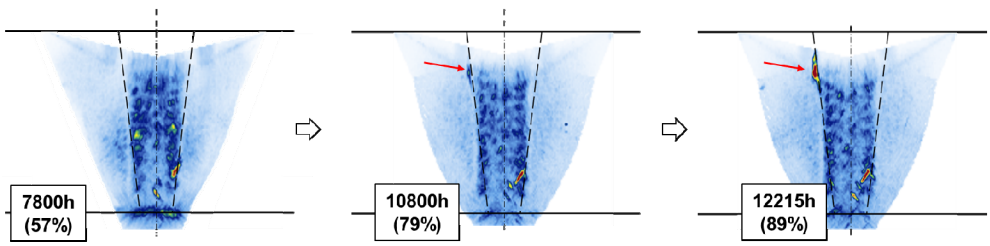

Figure 5 Results of PAUT on the side surface of creep interrupted specimens.

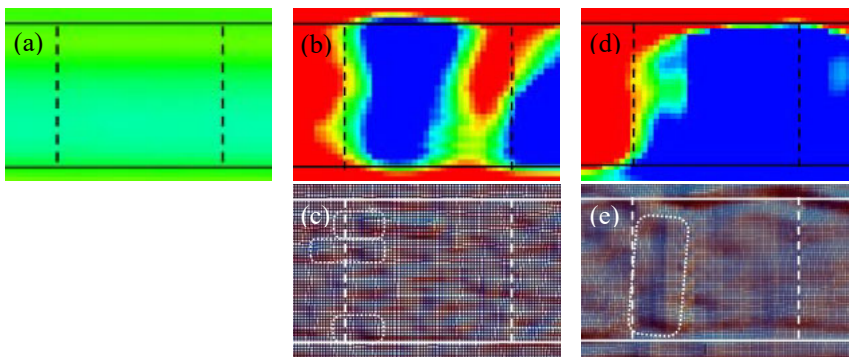

Figure 6 Result of ECT・HTS-dc-SQUID on outer surface of creep interrupted specimen. (a) before creep, (b) t=12215h, (c) t=13215h, (d) contour image of (c)

The results of ECT•HTS-dc-SQUID for the specimen interrupted for 12,215 and 13,215 h are shown in Fig. 6. High and low areas of detection intensity are observed around the creep damage. Figure 6 shows the detection intensity on the surface corresponding to the outer surface of the pipe. The high and low areas of detection intensity were confirmed near the fusion boundary at the left-hand side of the specimen, which may correspond to the creep damage. In this case, creep damage was detected between 79% and 89% of the creep life. Considering that the measurement results of ECT•HTS-dc-SQUID were affected by ECT, we are working to improve the sensitivity of ECT.

Microstructure on surface

Figure 7 shows the optical microscopy observation results of the replica from the side surface of the specimen interrupted for 7,800, 10,800, and 12,215 h. The location of the replica was at a depth of about 4 mm from the outer surface in HAZ. Creep voids were clearly observed in HAZ after creep for 7,800 h. The number of creep voids increased with an increase in the creep time. However, after creep for 12,215 h, a very small number of creep voids were observed on the replica obtained from the specimen surface corresponding to the outer surface of the pipe. AFM observation was also used to detect creep damage for the surface. A small number of creep voids were detected even after creep for 12,215 h corresponding to 99% of the creep life. For actual components, PAUT is suitable for the detection of creep damage because it can detect creep damage from the outer surface of the pipe.

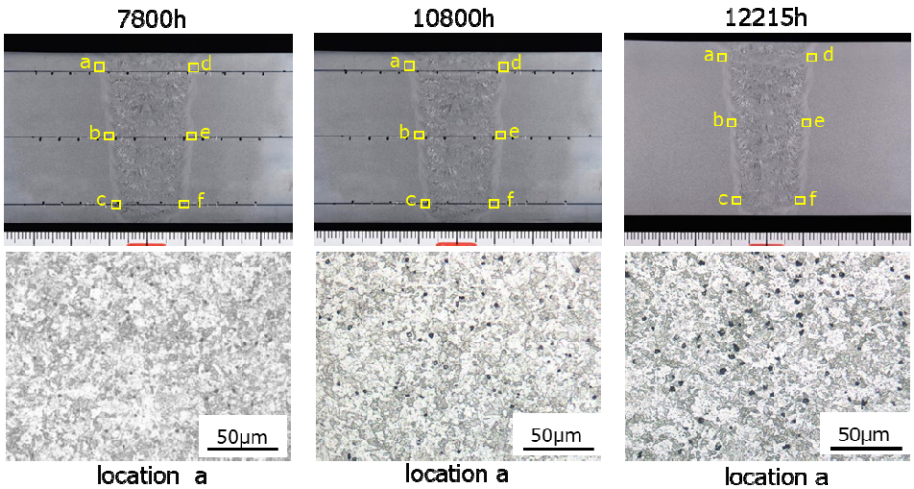

Figure 7 Optical micrographs of replica from the side surface.

Comparison of creep damage detection method

Table 4 summarizes the results of the creep damage evaluation by PAUT, ECT•HTS-dc-SQUID and the replica (OM and AFM). PAUT detected creep damage between about 60% and 80% of the creep life. In the case of ECT•HTS-dc-SQUID, creep damage was detected between about 80% and 90% of the creep life. Creep voids were observed on the replica from the outer surface just before creep rupture. PAUT was able to detect the creep damage at a relatively low creep life ratio compared with ECT•HTS-dc-SQUID.

Creep tests at 600°C under 60 MPa and 625°C under 40 MPa are ongoing for the next nondestructive testing. The time to rupture is expected to be 100,000 h under the test conditions. Creep damage evaluation using the replica from the outer surface will be attempted for the creep

specimens under the conditions mentioned above because creep damage can be quantitatively evaluated based on the observation of the creep voids for the replica.

Table 4 Summary of nondestructive testing.

Specimen 2-2			2400h 19%	5400h 44%	7800h 63%	10800h 87%	12215h 99%	
Inside	PAUT	Setting A	–	–	–	●	●	
		Setting B	–	–	–	●	●	
Surface	Replica (OM)		–	–	–	–	●	
	Replica (AFM)		–	–	–	–	●	
Specimen 3-2			2400h 18%	5400h 40%	7800h 57%	10800h 79%	12215h 89%	13215h 97%
Inside	PAUT	Setting C	–	–	–	●	●	●
		Setting D	–	–	–	●	●	●
	ECT・HTS-dc-SQUID		–	–	–	–	△	●
Surface	Replica (OM)		–	–	–	–	–	–

(● : detection, △: signal, – : no detection)
Surface : corresponding to the outer surface of pipe

Strain measurement

Figure 8 presents schematic drawings of the capacitive strain sensor and laser displacement meter. For the capacitive strain sensor, the strain was continuously measured during creep exposure. In the case of the laser displacement meter, the strain was measured after the creep test, which means that the measurement was not continuous. The relationship between the strain and the creep time is shown in Fig. 9. The strain obtained by the extensometer, capacitive strain sensor, and laser displacement meter gradually increased with an increase in the creep time. However, there was a large difference in the strain value among the three measurement methods. The gauge length for the extensometer, capacitive strain sensor, and laser displacement meter was 200, 95, and 103 mm, respectively. The gauge length included the base metal, HAZ, and weld metal for all three methods. However, the volume of the base metal in the gauge length was not the same for the three methods. Therefore, the strain may be different among the methods as shown in Fig. 9. It was confirmed that there was no large difference in the creep rate estimated by the extensometer and the capacitive strain sensor. Consequently, strain measurements by the capacitive strain sensor and laser displacement meter can be used to assess the residual life of actual components.

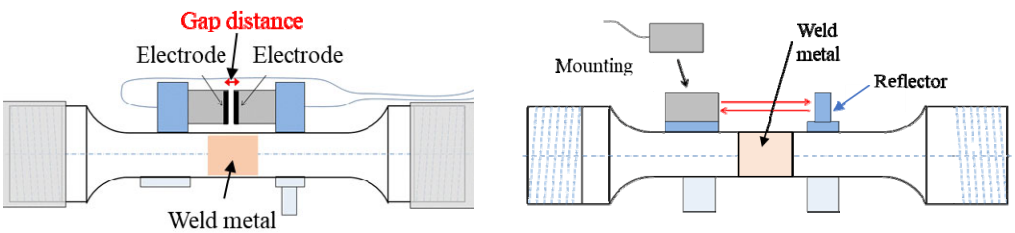

Figure 8 Schematic drawings of capacitive strain sensor (left) and laser displacement meter (right).

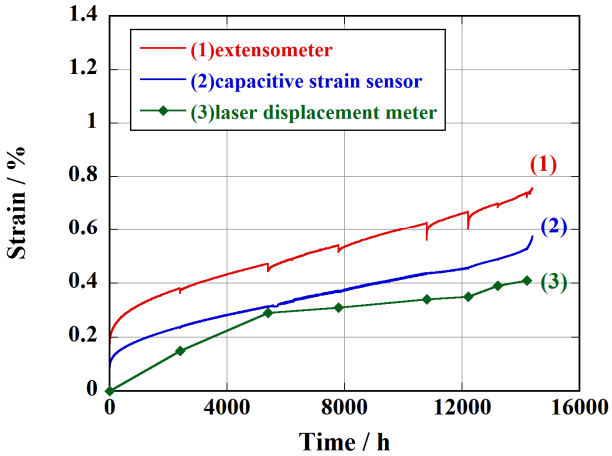

Figure 9 Creep curves by extensometer, capacitive strain senor and laser displacement meter.

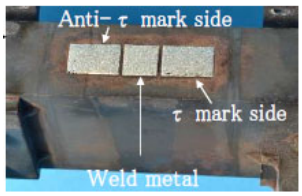

Figure 10 Appearance of platinum markers on specimen surface.

Figure 10 shows the platinum markers attached to the surface of the creep specimen for SPICA strain measurement. The platinum markers were used for the weld metal region and the area including the base metal and HAZ region. The distribution of axial SPICA strain for the creep interrupted specimens is shown in Fig. 11. The strain was already detected in HAZ after creep exposure for 2,400 h corresponding to 17% of the creep life. The strain in HAZ gradually increased with an increase in the creep time. No large change in the strain was observed in the weld metal compared to the HAZ region. Figure 12 shows the relationship between the average axial strain in HAZ and the creep time. The average strain monotonously increased during creep exposure. The accumulation of strain in HAZ may be one reason for the Type IV fracture. Therefore, the SPICA strain measurement in HAZ can be used to assess the residual life of actual components.

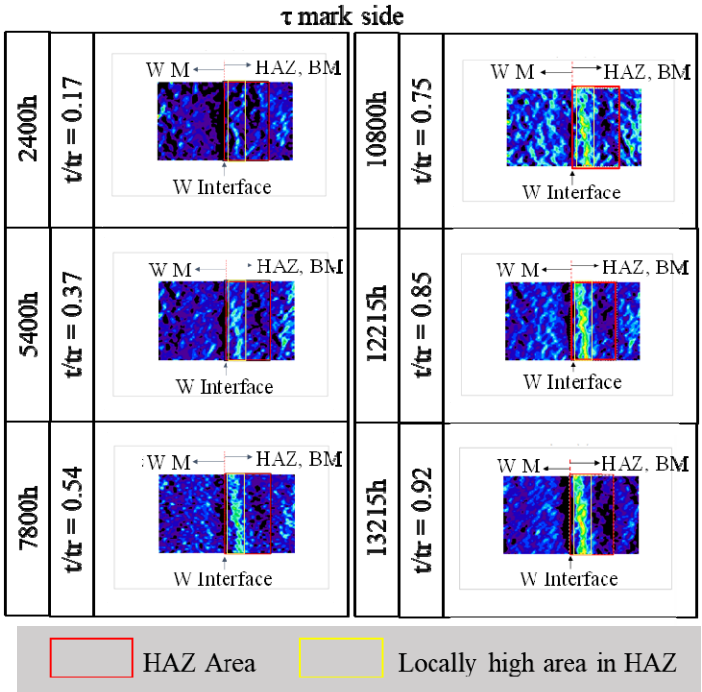

Figure 11 Change in distribution of axial SPICA strain during creep exposure.

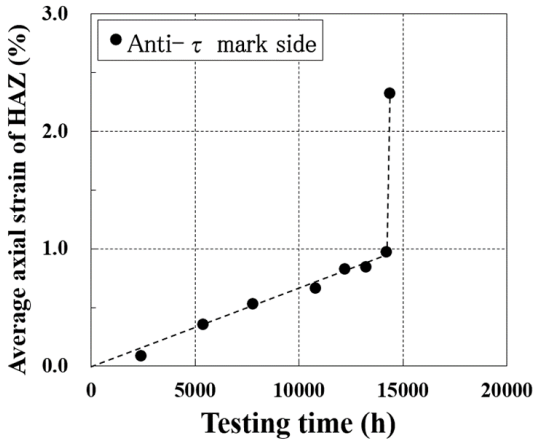

Figure 12 Change in average axial strain in HAZ during creep exposure.

CONCLUSIONS

Phased array ultrasonic testing (PAUT), eddy current testing with high-temperature superconductor, direct current, and superconducting quantum interference device (ECT•HTS-dc-SQUID), observation of replica were conducted to detect creep damage of Grade 91 steel welds. The results are summarized as follows.

1. PAUT detected creep damage between 60% and 80% of the creep life. In the case of ECT•HTS-dc-SQUID, creep damage was confirmed between 80% and 90% of the creep life.
2. Creep voids were detected just before creep rupture for the replica obtained from the specimen surface corresponding to the outer surface of the pipe.
3. There was no large difference in the creep deformation behavior for the extensometer, capacitive strain sensor, and laser displacement meter. Therefore, the capacitive strain sensor and laser displacement meter are useful for assessing the residual creep life of actual components.
4. The SPICA strain was detected in HAZ after creep exposure for 17% of the creep life. The SPICA strain in HAZ gradually increased during creep exposure. Therefore, the measurement of SPICA strain is a useful method for evaluating creep strain for residual life assessment.

REFERENCES

[1] M. Yaguchi, M. Kanai, K. Kako and S. Yamada, “Development of Remaining Life Assessment Method and Its Application to 9Cr Steel Pipe in Power Plants,” Thermal and Nuclear Power, Vol. 73, No. 2 (2022), pp. 171–177.
[2] H. Kushima, K. Kimura and F. Abe, “Degradation of Mod.9Cr-1Mo Steel during Long-term Creep Deformation,” Tetsu-to-Hagane, Vol. 85, No. 11 (1999), pp. 841–847.
[3] K. Kimura and M. Yaguchi, “Re-Evaluation of Long-term Creep Strength of Base Metal of ASME Grade 91 Type Steel,” Proceedings of the ASME 2016 Pressure Vessels and Piping Conference, Jul. 17–21, 2016.
[4] ASME Boiler and Pressure Vessels Code, Section II. A-2019.
[5] J. A. Francis, W. Mazur and H. K. D. H. Bhadeshia, “Type IV cracking in ferritic power plant steels,” Mater. Sci. Tech., Vol. 22, No. 12 (2006), pp. 1387–1395.
[6] S. J. Brett, “UK experience with modified 9%Cr (grade 91) steel,” Energy Mater., Vol. 2, No. 2 (2007), pp. 117–121.

[7] Y. Shioda, N. Saito, T. Tanoue, K. Nomura and K. Kubushiro, “Creep Damage Assessment of Gr. 91 Steel Welds by UPA Method,” J. Soc. Mater. Sci., Japan, Vol. 70, No. 2 (2021), pp. 177–183.
[8] H. Fukutomi, S. Nishinoiri and T. Ogata, “Applicability of Ultrasonic Testing of Type IV Damage in High Cr Alloy Steel Welds,” CRIEPI Research Report, No. 07003 (2008).
[9] T. Ohtani, T. Honma, Y. Ishii, M. Tabuchi, H. Hongo and M. Hirao, “Creep-Induced Nonlinear Ultrasonic Change in ASME Gr.91 Steel Welded Joint,” J. Soc. Mater. Sci., Japan, Vol. 66, No. 2 (2017), pp. 114–121.